TRANSACTIONS OF THE INSTITUTE OF FLUID-FLOW MACHINERY

No. 133, 2016, 145–162

Roman Rusanov[a*], Łukasz Jędrzejewski[a], Piotr Klonowicz[a], Grzegorz Żywica[a]
Piotr Lampart[a], A. Rusanov[b]

Design and performance study of a small-scale waste heat recovery turbine

[a] Institute of Fluid Flow Machinery, Polish Academy of Sciences, 80-231 Gdańsk, Fiszera 14, Poland
[b] A.N. Podgorny Institute of Mechanical Engineering Problems National Academy of Sciences of Ukraine, Kharkov, Ukraine

Abstract

The paper presents the design process of a radial-axial turbine working with SES36 working fluid. First, the mean-line design process is performed and then the geometry is developed. In the next stage the numerical verification is performed taking into account the real properties of the working fluid. The properties are implemented via a look-up table and by a modified Benedict-Webb-Rubin equation of state. The presented turbine is characterized by a very small stator outflow angle which is about 4.5° but despite this small value, the efficiency of the machine is relatively high and equal to about 88%. The influence of internal leakages has also been investigated.

Keywords: Cogeneration unit; Low-boiling working media; Numerical method; Turbine; Radial-axial stage

1 Introduction

A promising direction of development of energy-saving technologies for Europe is application of small power cogeneration plants operating with the low-boiling working media organic Rankine cycle (ORC), [1–4]. Such systems can also be used to utilize low-temperature waste heat, and work with renewable fuels – various

*Corresponding Author. Email adress: rrusanov@imp.gda.pl

types of biomass. The turbine is an important element of such cogeneration plants. The peculiarity of these turbines is their usually relatively small size, which complicates the task of achieving an acceptable level of gas-dynamic efficiency.

2 Plant layout. The initial data for the creation of a turbine

The ORC systems are similar to the steam cycles used in the large power industry. The fields of application of both technologies are roughly shown in Fig. 1 [5].

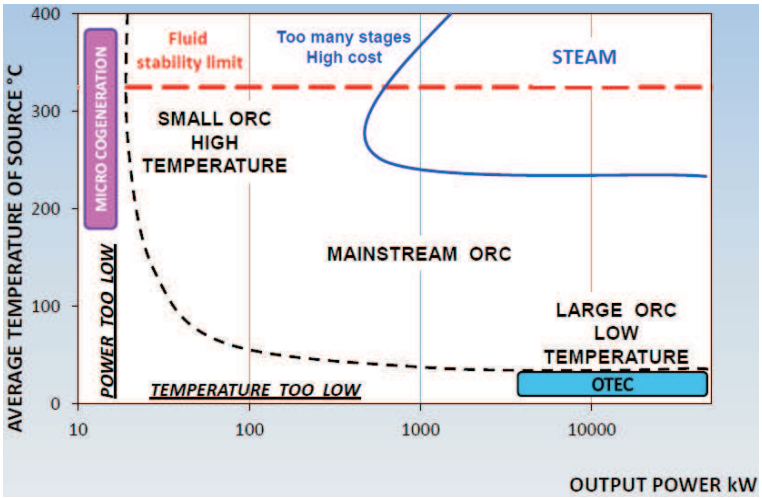

Figure 1: Fields of application of ORC systems and traditional steam systems [5].

The Institute of Fluid Flow Machinery, Polish Academy of Sciencies (IMP PAN) has built a combined gas-vapour cycle with the nominal power of about 400 kW and a high electrical efficiency. The primary generation unit is an internal combustion engine fuelled by natural gas which can also be fuelled by biogas and syngas in real applications and distributed cogeneration. At least two variants of such a system can be considered. For example, the ORC itself can work for cogeneration and accept both the exhaust heat and heat from the engine cooling loop. Alternatively, the ORC can work to produce only electrical power while the heat from the engine's cooling loop can directly be used for heating.

The system build at IMP PAN makes use of the second option. The schematic of the cogeneration plant and its photographs are shown in Figs. 2 and 3. As a working fluid, the substance SES36 has been used. The medium delivering

the heat from the engine exhaust to the ORC is a high temperature thermal oil Veco 5HT. The heat from the engine is transferred to the oil in a heat exchanger and then delivered to the preheater and the evaporator. The working fluid is evaporated and directed to the expansion unit coupled with the electrical generator. After the expansion process and transferring heat in the regenerator the fluid is directed to the condenser. The condenser transfers the remaining working fluid heat to the mixture of the water and glycol.

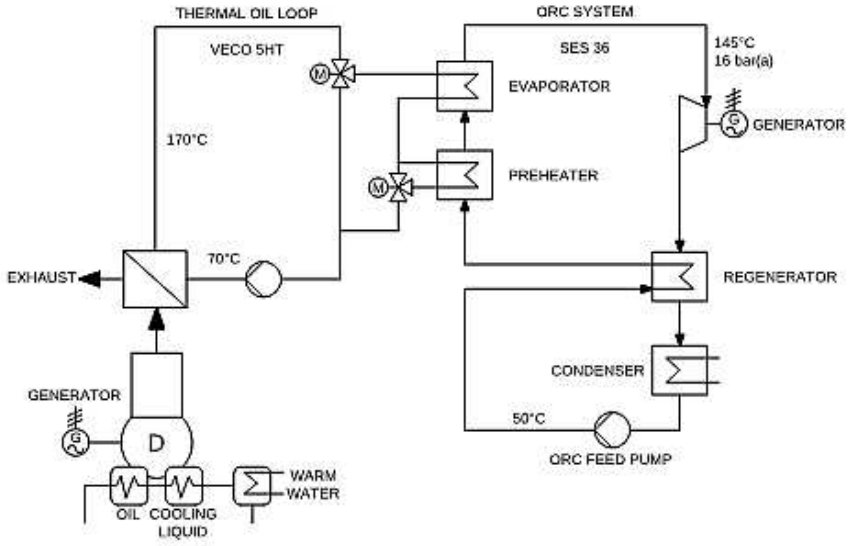

Figure 2: Schematic of the cogeneration plant with a combustion engine topped by an ORC cycle (D – combustion engine, M – valve control.)

3 Justification of the radial-axial turbine choice

The turbines characterized by the radial-axial direction of flow in many cases seem to be an attractive design solution. One of the main reason of using this type of turbine stages is their high efficiency for small specific speed values. Small values of this parameter result from small volume flow rate flowing through a device. Such situation takes place for example in small gas turbines or turbochargers [6]. The ORC systems are an alternative for traditional Rankine cycles but in fact ORC becomes really competitive for small power applications where the efficiency is not the most important factor and other characteristics such as simplicity, compact size and low investment costs are desirable. Small volume flow rates result

Figure 3: The combined gas/vapour (ORC) power plant: internal combustion engine from MAN (top left), heat recovery boiler (bottom left), 40 kW ORC system (right).

not only from the small scales of the systems. The fluids used in ORC plants have large particles which leads to large densities. Large density means small specific volume hence small volume flow rates. The tendency of using turbines of radial-axial direction of the flow in ORC systems can be found in many publications. All of them underline relatively high efficiencies of the small power machines [7–11].

A well described example of a 30 kW turbogenerator with a radial-axial turbine has been presented by Kang [7]. Figures 4 and 5 show the 3D model and a photograph of the device. The measured power and efficiency near the design point were found at 32.7 kW and 78.7%, respectively. It must be noted that this is the electrical efficiency of the turbogenerator which besides the turbine internal losses takes into account the shaft and disc friction losses, mechanical losses and electrical losses. In comparison with other small ORC turbines described in the literature this value is considered high [12,13].

Good parameters of radial-axial stages were one of the reasons why this kind of design was applied in the case of a turbogenerator working with the Solkatherm SES36 fluid at IMP PAN. This fluid is an azeotropic mixture [14], its thermodynamic parameters – both in 0D and computational fluid dynamics (CFD) simulations – have been acquired from the CoolProp thermodynamic properties library [15].

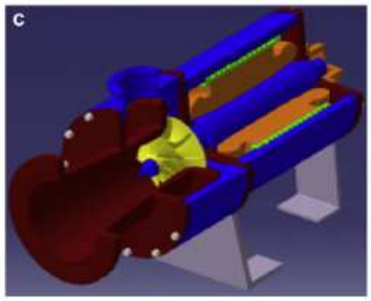

Figure 4: A 3D model of the turbogenerator designed for R245fa fluid [7].

Figure 5: A photograph of the R245fa turbogenerator [7].

4 Radial-axial single stream turbine

The most important design parameters of the turbine are shown in Tab. 1. In order to obtain a satisfying blade height at the stator a very small nozzle outflow angle α_1 was set equal to 4.4°. The velocity triangles for the stage have been presented in Fig. 6 and the main dimensions of the stage can be found in Fig. 7. The flowpath geometry was designed in the BladeGen software which belongs to the Ansys software package [17]. The designed nozzle (Fig. 8) has a convergent geometry despite supersonic character of the flow at the outlet. The reason for that is a relatively low Mach number which is equal to 1.33. For these conditions a convergent-divergent nozzle gives negligible efficiency benefit [16]. The stator and rotor assembly as a 3D model has been shown in Fig. 9.

Table 1: SES36 turbine design parameters.

Inlet pressure	1.464 MPa(abs)
Inlet temperature	414.15 K
Outlet pressure	0.22 MPa(abs)
Mass flow rate	1.22 kg/s
Rotational speed	15000 rpm

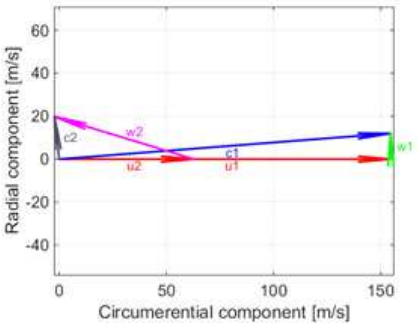

Figure 6: Velocity triangles of the SES36 turbine stage.

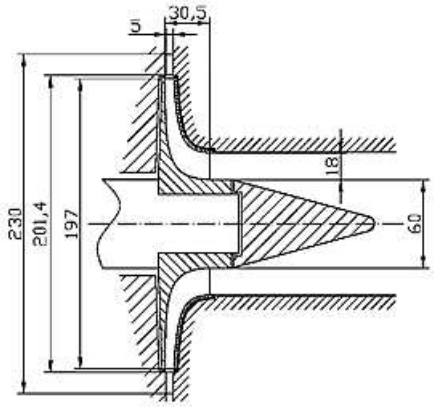

Figure 7: Main dimensions of the stage.

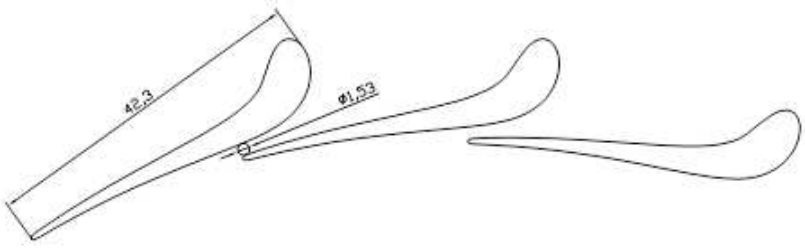

Figure 8: Stationary blade row of the designed stage.

The 3D simulations were performed in a commercial code Ansys CFX [17]. The whole computational domain consisted of 0.8 million nodes. The applied turbulence model was k-ω SST. The set of boundary conditions included the total parameters at the inlet and the static pressure at the outlet, also the inlet turbulence intensity. The summary of the 0D and CFD calculations has been presented in Tab. 2.

It turns out that despite the supersonic character of the flow and small stator angle, the efficiency of the stage is relatively high and equal to 88% (according to 3D results). This value does not include the internal leakage losses. Some complimentary distributions of the Mach number and velocity vectors have been shown in Figs. 10 and 11.

Figure 9: 3D model of the rotor and stator assembly.

Table 2: Results of the performed computations, part I.

Model 0D		Model 3D		Number of blades		Torque	Rotational speed
P [kW]	η [-]	P [kW]	η [-]	stator	rotor	T [Nm]	n [rpm]
29.4	0.86	30.2	0.88	22	15	19.23	15 000

Table 3: Results of the performed computations, part II.

Inlet pressure	Pressure between the blade rows	Outlet pressure	Inlet temperature	Temperature between the blade rows	Outlet temperature
p_0 [kPa]	p_1 [kPa]	p_2 [kPa]	T_0[K]	T_1 [K]	T_2 [K]
1464	492	220	414.15	386.45	370.1

5 Radial-axial double stream turbine

The main disadvantage of the single stream radial-axial construction is a significant axial thrust. This shortcoming is absent in the double stream turbine, in which the flow starting from the radial section is divided into two symmetrical axial flows (in different directions). This kind of design can be realized in two variants – back-to-back rotor wheels and front-to-front rotor wheels (this variant

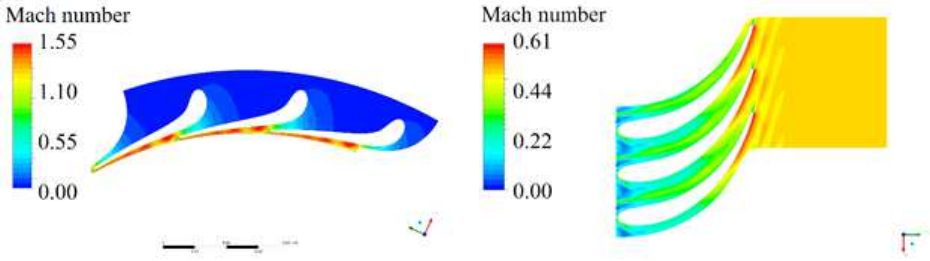

Figure 10: Relative Mach number (50% of span; left – stator, right – rotor.

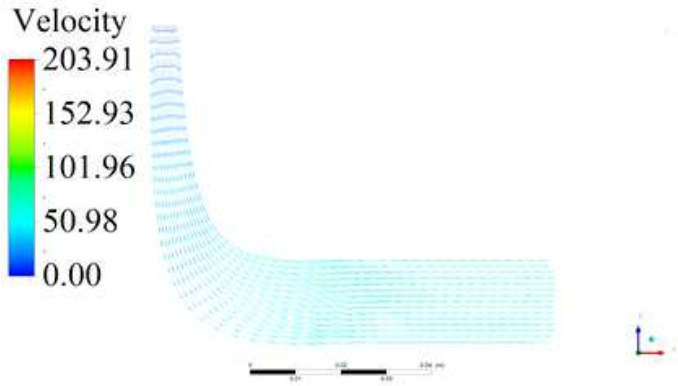

Figure 11: Velocity vectors in the rotor averaged at meridional surface.

is axially longer as there must be space between the rotors to form the outlets).

Figure 12 presents a view of the flow part and Tab. 4 shows the main characteristics of the double stream radial-axial turbine (single side). 3D calculations of the designed flow part were performed using the software package IPMFlow [12]. The calculation is performed on the grid with a total number of more than 1 million cells (about 500 thousand of cells in one row) using the Benedict-Webb-Rubin equation of state with 32 members [18].

Figures 13 and 14 show a visualization of the flow path, whereas Tab. 5 gathers main integral characteristics obtained from 3D calculations. Despite the fact that the flow part consists of a single stage, which operates at a high thermal gradient, there is a favorable flow pattern. The maximum value of the Mach number in the whole of the flow part is less than 2, there are no strong shocks and flow separations. The proposed flow part has a high gas-dynamic efficiency, its internal efficiency is 88.5 %. Despite the advantageous properties of the double stream

Table 4: The geometrical characteristics of the radial-axial flow part.

r_{in}, stator	r_{out}, stator	l_{in}, stator	l_{out}, stator	z, stator
100 mm	86.0 mm	3 mm	3 mm	41
r_{in}, rotor	$r_{mid.out}$, rotor	l_{in}, rotor	l_{out}, rotor	z, rotor
81 mm	36.3 mm	3 mm	16 mm	16

where r_{in} – inlet radius, r_{out} – outlet radius, $r_{mid.out}$ – outlet mid radius, l_{in} – blade inlet height, l_{out} – blade outlet height, z – number of blades.

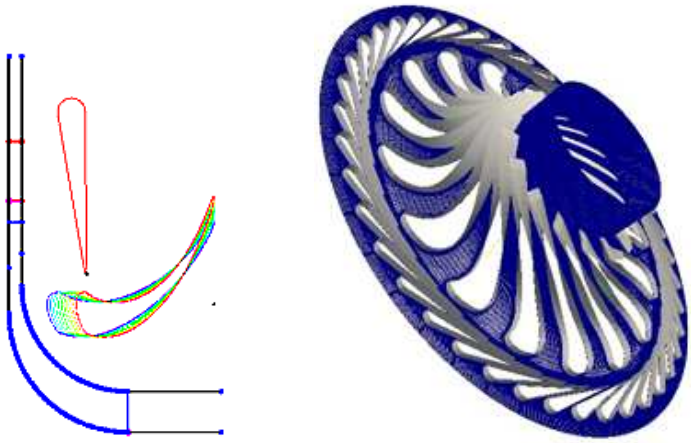

Figure 12: Relative Mach number ($x/l = 0.5$); left – stator, right – rotor.

geometry the single stream variant has been selected for actual manufacturing as it is a cheaper and simpler solution.

Table 5: The main integral characteristics of the flow part.

Inlet pressure p_1 [kPa]	Inlet temperature T_1 [K]	Temperature between blade rows T_2 [K]	Rotor inlet absolute velocity c_1 [m/s]	Outlet absolute velocity c_2 [m/s]	Rotor inlet relative velocity w_1 [m/s]	Outlet relative velocity w_2 [m/s]	Stage power P [kW]	Stage efficiency η [-]
440.5	394.67	379.77	152.1	29.9	26.7	72.8	30.1	0.885

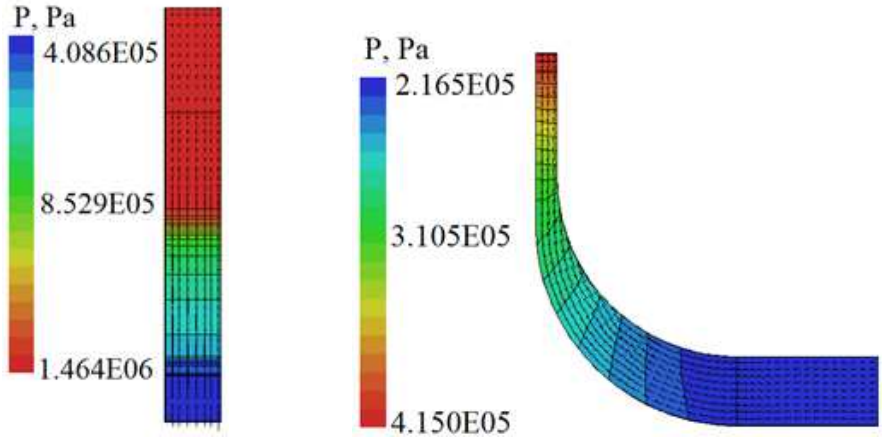

a b

Figure 13: Velocity vector and pressure contours in the average meridional section: a – stator; b – rotor.

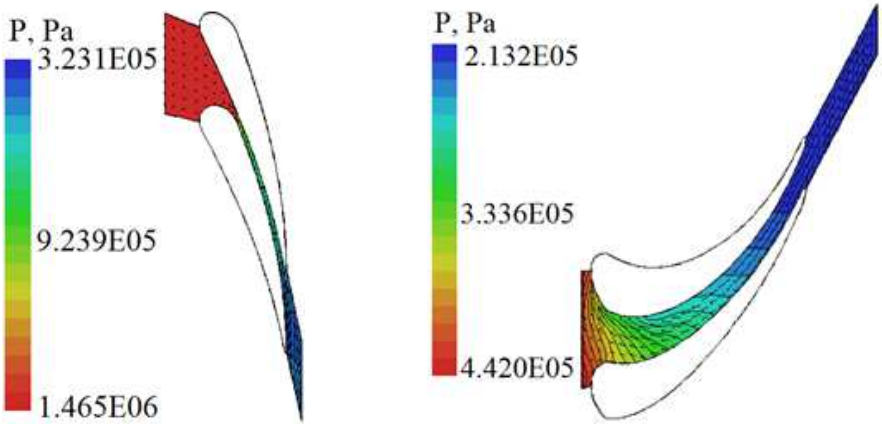

a b

Figure 14: Velocity vector and pressure contours in the middle tangential section: a – stator; b – rotor.

6 Mechanical design

High rotational speed and significant axial thrust (reaction turbine) require an adequate bearing system [19,20]. One of the best choice would be to use oil lubricated slide bearings. Unfortunately, one of the design condition was a hermetic casing in order to minimize the working fluid loss. Lubrication with oil would also

require a special mechanical sealing and oil separation.

Using magnetic bearings would be an option but this kind of bearing system is the most expensive and does not pay off in a small machine. Another option would be to use static or dynamic (e.g. foil) bearings but the drawback of this solution is its relatively small capacity, which in the case of a reaction turbine (significant axial thrust) requires a balancing piston. A balancing piston is a device that increases the internal leakage loss and requires a longer rotor (shaft) which is particularly undesirable in an overhang design.

Some companies apply slide bearings lubricated by a liquid fraction of the working fluid (greater capacity) but they require an additional cooling cycle in order to avoid local boiling in the lubrication film.

All of the above methods could be considered in a commercial application but in the presented laboratory tests, the study of the flowpath was the priority. For this reason it was decided to apply angular contact ball bearings which are not that durable but offer high stiffness, replacement simplicity, high capacity and are easily available. The 3D ,pdel of the turbogenerator designed at IMP PAN is shown in Fig. 15 and the assembly drawing of the whole turbogenerator has been presented in Fig. 16.

Figure 15: 3D model of the SES36 turbogenerator.

7 Internal leakages

The aspect of the internal sealings should be considered not before but after the mechanical design concept is derived, especially in small machines in which the simplicity comes first.

All parts of the casing, generator together with the stator-rotor section and

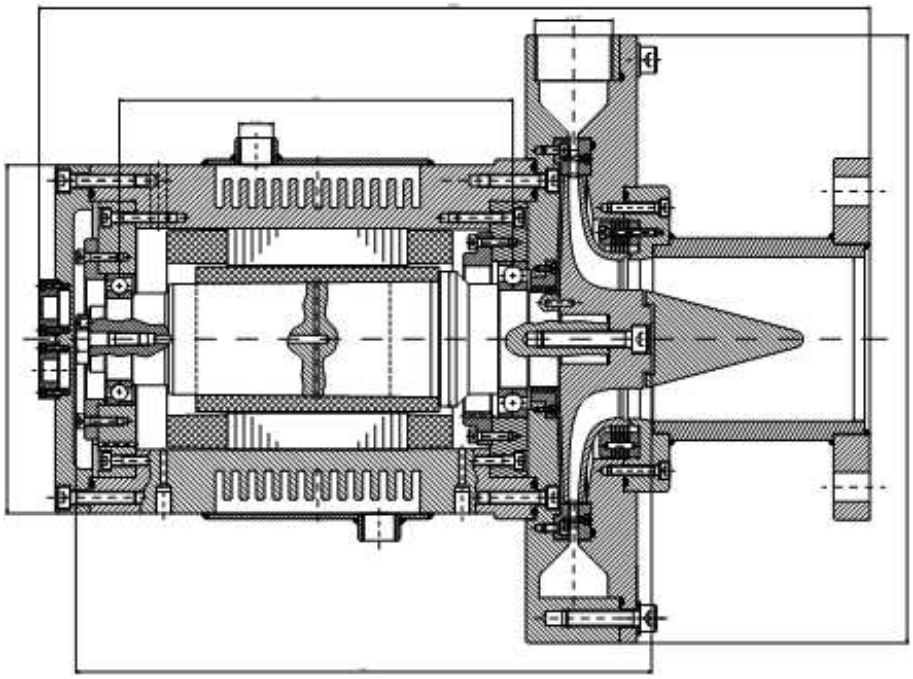

Figure 16: Assembly drawing of the SES 36 turbogenerator.

outlet part, were designed as a vertical split case. This type of design is more tight but it has some limitations for sealing solution application. The axial assembly causes that the full labyrinth sealing cannot be applied. A serial labyrinth must be used instead. This type of sealing with one wall smooth is much less efficient than the full labyrinth because of the fact that kinetic energy of flow passing the gap is not fully decreased within one single sealing chamber [21].

Several variants of a serial labyrinth seal of the rotor were analysed. More sophisticated solutions like coal sealing, abradable sealing or brush sealing were not analysed. The outlet part of rotor shroud was specially shaped to be able to work with labyrinth sealing. The sealing section was designed as a removable part, mounted directly to the outlet pipe, Fig. 17. This solution gives more possibilities for making any changes in the sealing method by replacing the whole unit. All analysed variants of the rotor sealing are presented in Fig. 18.

The gap thickness was established as 0.25 mm (a radial clearance). The single labyrinth thickness is equal to 0.5 mm. A fully theoretical solution for this type of sealing in not possible [21], therefore there are several methods that use correlations and data from experimental works. In general the flow through the

sealing gland can be described as follows:

$$m_n = A_n \Phi \sqrt{\frac{p_1}{\eta_1}}\,, \tag{1}$$

where: m_n – steam mass flow rate through the sealing, A_n – effective profile of the gap, p_1 – static pressure before the sealing section, η_1 – specific volume of steam before the sealing section, and z – number of seals. Effective profile of the gap is defined as

$$A_n = \alpha \pi d s\,, \quad \Phi = \Phi\left(\frac{p_2}{p_1}, z\right)\,, \tag{2}$$

where α – coefficient of flow in gap, d – shaft diameter, s - -nominal gap clearance.

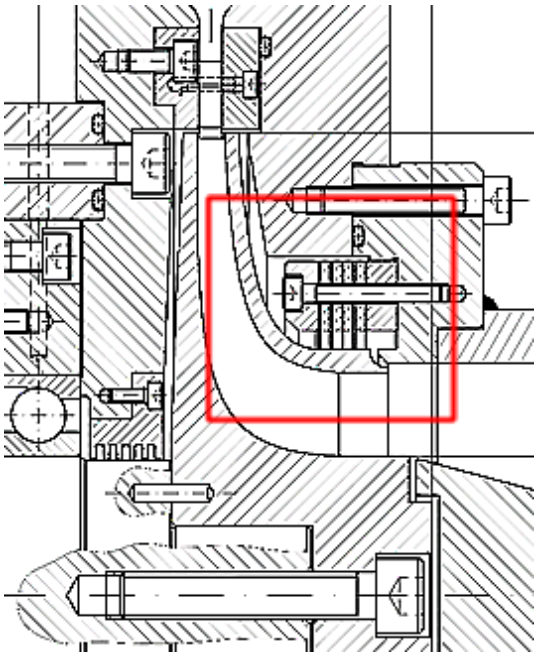

Figure 17: Rotor serial labyrinth sealing mounted to the outlet section.

The function of pressure drop p_2/p_1 (p_2 – pressure at the sealing outlet) includes the information about the α coefficient of flow and it is dependent on the shape of the labyrinth seal and the a/s ratio, where a is the distance between the seals. Figure 19 shows a chart with the flow function shapes for serial labyrinth

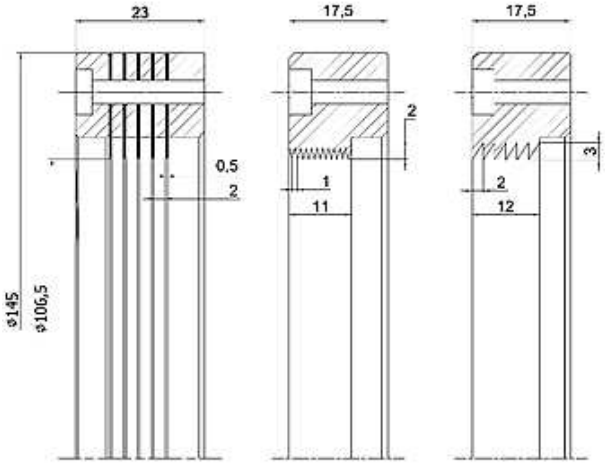

Figure 18: Geometry of the proposed sealing rings, 3 considered variants.

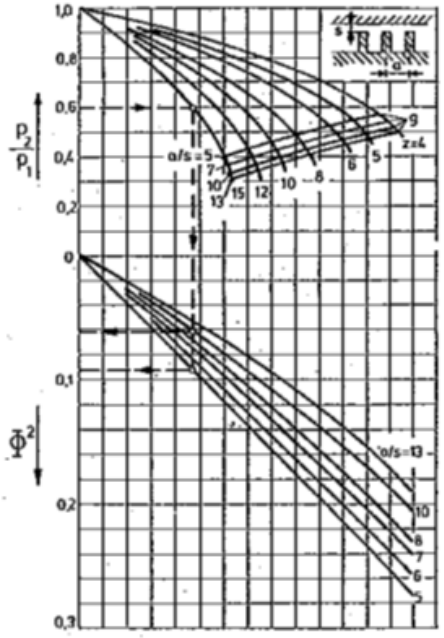

Figure 19: Function of flow for the serial labyrinth sealing.

sealings, data comes from experimental research [21]. The values assumed in the calculations and the results for different variants of seals are summarised in Tab. 6.

Table 6: Parameters and values assumed during sealing calculations.

No.	Value	Symbol	Units	Variant 1	Variant 2	Variant 3	Example
1	Number of blades	z	–	5	11	6	12
2	Gap clearance	s	m	0.00025	0.00025	0.00025	0.00025
3	Distance between blades	a	m	0.002	0.001	0.002	0.003
4	a/s ratio	a/s	–	8	4	8	12
5	Flow coefficient in gap	α	–	0.7	0.7	0.7	0.7
6	Shaft diameter	d	m	0.106	0.106	0.106	0.106
7	Effective area of flow	A_n	m^2	5.83×10^{-5}	5.83×10^{-5}	5.83×10^{-5}	5.83×10^{-5}
8	Pressure at the sealing inlet	p_1	Pa	492 000	492 000	492 000	492 000
9	Pressure at the sealing outlet	p_2	Pa	220 000	220 000	220 000	220 000
10	Speciffic volume before sealing	ν	m^3/kg	0.0312	0.0312	0.0312	0.0312
11	Pressure ratio	p_2/p_1	–	0.447	0.447	0.447	0.447
12	Square of the flow function value	Φ^2	–	0.19	0.16	0.17	0.08
13	Flow function value	Φ	–	0.436	0.4	0.412	0.283
14	Mass flow of the leak	m_n	kg/s	0.101	0.093	0.095	0.065

In each sealing geometry seals were assumed sharp. Results show similar values of leak. It is possible to obtain better results, to decrease the flow rate of leak but the number of seals and the distance between them should be increased, or the gap clearance should be decreased. More seals means that the sealing module and the rotor shroud would be longer. This scenario is limited by strength and dynamic conditions. It is important to realise that this method can introduce some errors into the values of flow because this algorithm is not dependent on the rotor rotational speed and the real shape of the labyrinth sealing. The calculations were verified by another method, where leakage mass flow rate is extracted directly like for full labyrinth sealing, than a correction coefficient is introduced, suitable for proper seal geometry [22]. The formula

$$G = 0.933\alpha\mu\gamma F_p\sqrt{\frac{p_1}{\nu_1}}\,, \tag{3}$$

takes into account geometry of the seal where: α – relative flow through the sealing, function of number of seals and inlet-outlet pressure ratio, μ – coefficient

of leakage through the gap, dependent on the geometry of the seal (experimental data), ν – correction factor for half labyrinth sealing, function of number of seals and the coefficient of kinetic energy utilization by steam passing through following spaces between seals, F_p – geometrical area of the sealing gap.

The results from this algorithm are slightly different compared to the previous one and the mass flow rate is higher in each analysed case, Tab. 7. It is important to underline that both methods are based on empirically derived factors and averaged experimental data thus errors can be expected.

Table 7: Results from second algorithm.

Value	Symbol	Units	Variant 1	Variant 2	Variant 3	Example
Mass flow rate	m_n	kg/s	0.13	0.132	0.125	0.090

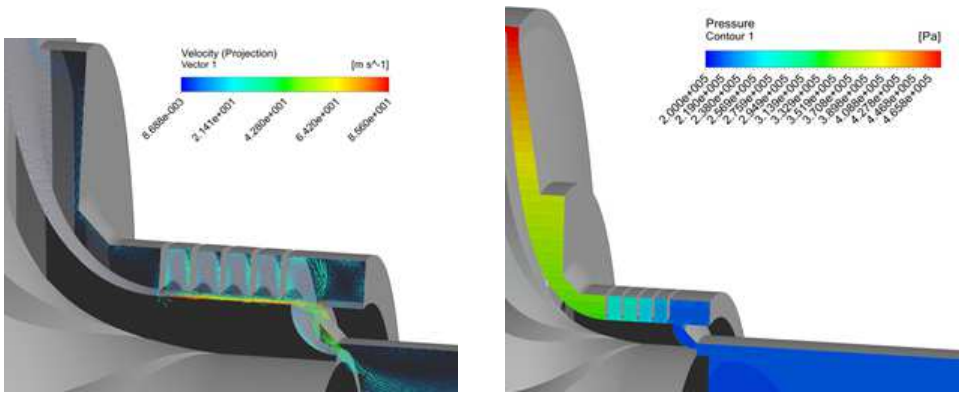

Figure 20: CFD results for the internal sealing domain.

In order to investigate the leakage by one more method a CFD analysis has been performed taking into account the labyrinth sealing domain (only for variant 1), Fig. 20. The obtained mass flow rate of the leakage is equal to 0.117 kg/s. This value is almost exactly between the results given by the two empirical methods. It must be seen, however, that the significant part of the pressure drop occurs also upstream of the labyrinth during the centripetal flow. This effect is caused by the radial equilibrium formed in this part of the domain as the fluid is in rotational motion. Thus, it can be concluded that if the CFD results are reliable, then the empirical methods underestimate the value of the leakage. What is more, the mass flow rate of the internal leakage is almost 10% of the total mass

flow rate through the machine. It means that the work done by the fluid on the rotor is almost 10% less than without the leakage and that corresponds to the similar drop in the efficiency.

8 Conclusions

A case study of a small turbogenerator design process has been presented. Two variants of radial-axial turbine flowpaths working with SES 36 fluid have been considered. Both variants reveal a relatively high gas dynamic efficiency equal to about 88% in each case. However, single stream turbine is preferable because it is a simpler design, cheaper to manufacture and safer if considered from the point of rotordynamics.

The concept of the mechanical design has been also briefly described, mainly from the point of view of the bearing selection. The set of angular contact ball bearings has been selected as an advantageous option from the point of view of a laboratory test rig.

The analysis of internal leakages has been described in more detail. It can be seen that the internal sealing is a crucial component, especially in small machines. Despite a relatively small radial clearance between the rotor and the casing labyrinth the internal leakage is about 10% of the main flow ratio. It corresponds to a similar drop in the turbine stage efficiency. Perhaps, for small cogeneration units more sophisticated sealing technologies could be beneficial.

Received in July 2016

References

[1] Duvia A., Gaia M.: *ORC plants for power production from biomasss from 0.4 to 1.5 MWe. Technology, efficiency, practical experiences and economy.* In: Proc. 7th Holzenergie Symp., ETH Zürich 2002.

[2] Mikielewicz J., Bykuć S., Mikielewicz D.: *Application of renewable energy sources to drive ORC mikro CHP.* In: Heat Transfer Renewable Sources of Energy (J. Mikielewicz, W. Nowak, A. Stachel, Eds.), 2006.

[3] Nowak W., Borsukiewicz-Gozdur A.: *ORC power plants as a means of utilisation of energy from low-temperature sources.* Czysta Energia **2**(2011), 32–35 (in Polish).

[4] Mikielewicz J., Mikielewicz D., Ihnatowicz E., Kaczmarczyk T., Wajs J., Matysko R. *et al.*: *Thermodynamic cycles of ORC micro power plants.* Wydawnictwo IMP PAN, Gdańsk 2013.

[5] Gaia M.: *30 years of organic Rankine cycle development.* In: Proc. First Int. Semin. ORC Power Syst., Delft 2011.

[6] Baljé O.E.: *A study on design criteria and matching of turbomachines: Part A – Similarity relations and design criteria of turbines*. J. Eng. Power **84**(1962), 1, 83–102, DOI:10.1115/1.3673386.

[7] Kang S.H.: *Design and experimental study of ORC (organic Rankine cycle) and radial turbine using R245fa working fluid*. Energy **41**(2012), 1, 514–524.

[8] Capata R., Hernandez G.: *Preliminary design and simulation of a turbo expander for small rated power organic Rankine cycle (ORC)*. Energies **7**(2014), 11, 7067–7093, DOI:10.3390/en7117067.

[9] Klonowicz P., Rusanov R., Rusanov A., Lampart P., Suchocki T., Surwiło J.: *Methods for design of radia-axial turbines for ORC cogeneration unit working with MDM*. Bull. NTU 'KhPI'. Ser. Power Heat Eng. Process. Equip. **16**(2015), 67–77.

[10] Klonowicz P., Surwiło J., Witanowski Ł., Suchocki T.K., Kozanecki Z., Lampart P.: *Design and numerical study of turbines operating with MDM asworking fluid*. Open Eng. **5**(2015), 485–499, DOI:10.1515/eng-2015-0050.

[11] Suchocki T., Lampart P., Klonowicz P.: *Numerical investigation of a GTM-140 turbojet engine*. Zesz. Nauk. Ciepl. Masz. Przepływowe – Turbomach. / Politech. Łódzka. **145**(2014), 115–116.

[12] Klonowicz P., Borsukiewicz-Gozdur A., Hanausek P., Kryłłowicz W., Brüggemann D.: *Design and performance measurements of an organic vapour turbine*. Appl. Therm. Eng. **63**(2014), 1, 297–303. http://www.sciencedirect.com/science/article/pii/S1359431113008065 (accessed Jan. 10, 2014).

[13] Harinck J., Pasquale D., Pecnik R., Colonna P.: *Three-dimensional RANS simulation of a high-speed organic Rankine cycle turbine*. In: Proc. First Int. Semin. ORC Power Syst. ORC 2011, Delft 2011.

[14] Solvay, Solkatherm§SES36, http://www.solvaychemicals.com/EN/products/Fluor/SOLKANE_Specialties/SolkathermSES36.aspx.

[15] Bell I.H., Wronski J., Quoilin S., Lemort V.: *Pure and pseudo-pure fluid thermophysical property evaluation and the open-source thermophysical property library CoolProp*. Ind. Eng. Chem. Res. **53**(2014), 2498–2508, DOI:10.1021/ie4033999.

[16] Craig H.R.M., Cox H.J.A.: *Performance estimation of axial flow turbines*. In: Proc. Inst. Mech. Eng. **185**(1970), 1, 407–424.

[17] ANSYS Academic Research, Lelease 16, 2014.

[18] Rusanov A.V., Lampart P., Rusanov R.A.: *Interpolation-analytical approximation of modified Benedict-Webb-Rubin equation of state for accounting of the real properties of working fluid in 3D calculations*. Compress. Energ. Mach. Build. (2014), 18–23.

[19] Kicinski J., Zywica G.: *The numerical analysis of the steam microturbine rotor supported on foil bearings*. Adv. Vib. Eng. **11**(2012), 2, 113–119.

[20] Zywica G., Drewczynski M., Kicinski J., Rzadkowski R.: *Computational modal and strength analysis of the steam microturbine with fluid-film bearings*. J. Vib. Eng. Technol. **2**(2014), 6, 543–549.

[21] Perycz S.: *Steam and gas turbines*. IMP PAN, Ossolineum, Wrocław 1992 (in Polish).

[22] Samojłowicz G., Trojanowski B.: *Steam turbines*. PWN, Warsaw 1957 (in Polish).